

NASA TECHNICAL NOTE



NASA TN D-2891

NASA TN D-2891

FACILITY FORM 602

N65-26654	
(ACCESSION NUMBER)	(THRU)
19	1
(PAGES)	(CODE)
	33
(NASA CR OR TMX OR AD NUMBER)	(CATEGORY)

GPO PRICE \$ _____
CRST/OTS PRICE(S) \$ 1.00

Hard copy (HC) _____

Microfiche (MF) .50

PERFORMANCE OF MULTIPLE-CHAMBER ARC HEATER WITH FOUR MAGNETICALLY SPUN DIRECT-CURRENT ARCS

*by Donald R. Boldman, James P. Campbell,
and Paul C. Simon*

*Lewis Research Center
Cleveland, Ohio*

PERFORMANCE OF MULTIPLE-CHAMBER ARC HEATER WITH
FOUR MAGNETICALLY SPUN DIRECT-CURRENT ARCS

By Donald R. Boldman, James P. Campbell, and Paul C. Simon

Lewis Research Center
Cleveland, Ohio

NATIONAL AERONAUTICS AND SPACE ADMINISTRATION

For sale by the Clearinghouse for Federal Scientific and Technical Information
Springfield, Virginia 22151 - Price \$1.00

PERFORMANCE OF MULTIPLE-CHAMBER ARC HEATER WITH FOUR MAGNETICALLY SPUN DIRECT-CURRENT ARCS

by Donald R. Boldman, James P. Campbell, and Paul C. Simon

Lewis Research Center

SUMMARY

A multiple-chamber arc heater incorporating four magnetically spun direct-current arcs was tested over a range of power levels and nitrogen flow rates to determine its value as a heater for hypersonic wind tunnels. Enthalpy levels, determined from energy balance measurements, ranged from 4000 to 6000 Btu per pound at a nominal pressure of 2.0 atmospheres and a nozzle throat diameter of 3/4 inch. The efficiency of the arc chamber ranged from about 45 percent at a power level of 600 kilowatts to about 30 percent at 1200 kilowatts. As in single-heater operation, the electrodes were the primary source of heat loss. At 1000 kilowatts the electrode heat loss was 47 percent of the arc power for the highest total nitrogen flow rate, 0.058 pound per second. The corresponding plenum and nozzle losses were 18 and 3 percent of the arc power, respectively.

Certain multiple-arc stability considerations are presented to show the importance of using a separate power supply for each arc heater in a multiple-chamber system. The reductions in the electrical fluctuations that can be realized by incorporating a series inductance in the circuit are indicated. In the case of magnetically spun arcs, the inductance can be obtained, conveniently, by connecting the field coil in series with the arc.

An attempt was made to correlate measured values of stagnation enthalpy with the values predicted on the basis of equilibrium sonic flow. The results indicated that the measured stagnation enthalpy was generally higher than that predicted for one-dimensional real-gas sonic flow by assuming either equilibrium or frozen subsonic expansion processes. The reason for this is unclear; however, the same general trend was noted in earlier investigations of single-arc heater performance.

Measured nozzle losses correlated well with the integrated values of calculated local heat-transfer rates based on laminar pipe flow theory.

INTRODUCTION

A need for simulating various aerothermodynamic phenomena occurring in high-speed flight and reentry has stimulated research in the field of high-powered arc discharges. Use of such discharges in wind-tunnel facilities provides a means of heating gases far beyond the melting point of the containment materials with negligible contamination of the working fluid. Numerous electrode configurations for the production of high-energy gas streams have been tested in the past 8 years to determine performance limits and gain a better understanding of the physical phenomena associated with the discharge. Large-scale arc tunnels (test-section areas greater than 1 sq ft) require heaters that are capable of supplying gas powers at megawatt levels. Problems arise in the attainment of these large powers as a result of power limitations inherent in the arc heater. Two approaches have been used to obtain higher powers from otherwise power-limited electrode configurations, namely, (1) application of geometric scaling techniques as in references 1 and 2, and (2) utilization of multiple electrodes (ref. 3) or heaters. Many of the problems associated with multiple-heater systems have been discussed in references 4 and 5. The multiple-heater approach has the advantage that high power can be attained with smaller arc heaters, for which performance data are more easily obtained. The physical complexity of the overall system is a major disadvantage.

The goal of this investigation was to determine the performance of a multiple-chamber arc heater utilizing the magnetically spun arc chamber configuration reported in reference 3 and to determine whether the clustering of arc heaters results in lowered enthalpy level and reduced heater efficiency.

SYMBOLS

A	area, sq ft
A*	geometric throat area, sq ft
d	diameter, ft
H _i	initial gas enthalpy (before heating), Btu/lb
H ₀	stagnation enthalpy, Btu/lb
I	current, amp
K	conversion factor
L	nozzle length, ft
\dot{m}	nitrogen flow rate, lb/sec

$\overline{Nu_d}$	Nusselt number based on diameter
P_a	arc power, $V_a I_a / 1000$, kW
Pr	Prandtl number, 0.7
P_0	stagnation pressure, lb/sq ft or atm
Q	total heat load, kW
\dot{q}	local heat-transfer rate, Btu/(sq ft)(sec)
R_b	ballast resistance in series with each arc, ohms
R_c	ballast resistance common to multiple-arc network, ohms
Re_d	Reynolds number based on diameter
R_g	ballast resistance common to multiple-arc network, ohms
$R_1, R_2 \cdots R_n$	resistance, ohms
V	voltage, volts
x	axial distance along nozzle, ft
Subscripts:	
a	arc
E	electrodes
g	generator
N	nozzle
P	plenum
T	total
Superscript:	
$-$	average

MULTIPLE-CHAMBER ARC HEATER

Support Equipment

The power supply for the multiple-chamber arc heater consisted of four direct-current generators, each rated at 600 volts and 1000 amperes and capable of supplying 720 kilowatts for durations of 5 minutes. The generators could be connected in parallel or used independently. Each generator contained a series ballast resistor capable of

providing stepwise variations in resistance between 0.15 and 0.33 ohm in 0.03-ohm increments.

The downstream static pressure used to attain sonic flow in the nozzle was obtained from a two-stage air ejector-exhauster system that provided pressures as low as 0.1 torr with no flow in the arc chamber. This system was based on the results of an investigation reported in reference 6.

A centrifugal pump delivered deionized water to the cooling passages of the heater and plenum from a 2500-gallon tank at the rate of 600 gallons per minute with a pump discharge pressure of 1000 pounds per square inch gage. The water was recirculated to the tank through a small heat exchanger. The capacity of this heat exchanger was insufficient to maintain a constant water inlet temperature during the tests; hence, a run was limited to about 10 minutes. The water flow rate and pressure level for each component were regulated by means of pneumatic control valves.

Arc Chamber

Important considerations in designing the four-chamber arc heater to utilize the total available electric power were as follows:

(1) In reference 3 it was indicated that, at atmospheric pressure, the current limit for the magnetically spun arc used in this investigation is approximately 1500 amperes (2000 amps if run times are limited to a few minutes), corresponding to an arc potential difference of about 200 volts. At higher current, a prohibitive amount of electrode erosion was encountered.

(2) Operation of coplanar radially symmetric multiple heaters, each having an axial magnetic field, requires an even number of heaters in order to prevent magnetic field cancellations. Cancellation of the field in the critical anode region would lead to severe erosion or burnout.

(3) The gas vortices created by the Lorentz force on the arc tend to cancel in the plenum if an even number of heaters is used, because the swirl directions oppose in diametrically opposite heaters and thus the flow conditions in the nozzle entrance region are improved.

(4) Experience has shown that continuous, well balanced operation of multiple-arc chambers powered by a single source is difficult to attain. (This problem will be discussed in greater detail in the section PERFORMANCE.) All tests, therefore, were conducted with equally powered arc chambers in which a separate generator was connected to each set of electrodes. The four arc chambers shared a common ground return line.

The photograph of the multiple-chamber arc heater in figure 1 shows the complexity

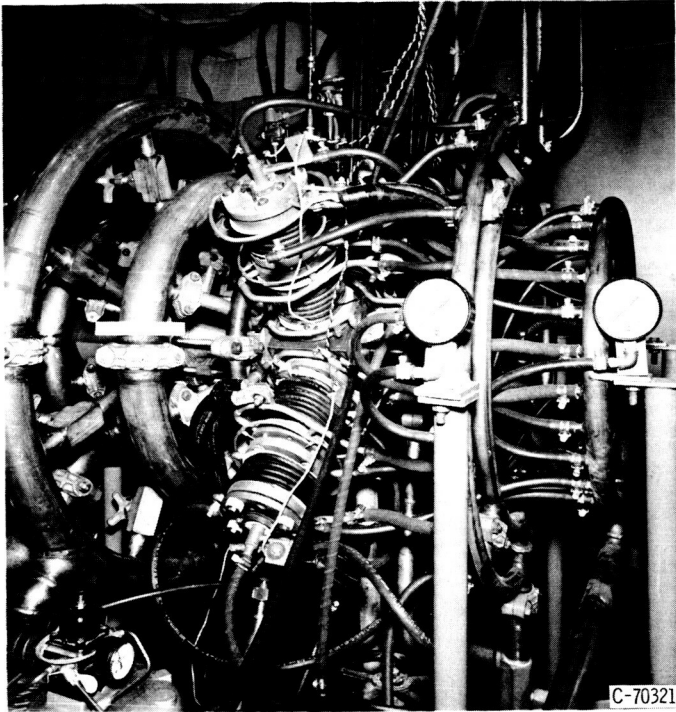


Figure 1. - Multiple-chamber arc heater showing two of four arc heaters.

of the system, particularly the numerous cooling-water connections. A schematic diagram is provided in figure 2. Four arc chambers of the type described in reference 3 were attached to a 5-inch-inside-diameter, 6-inch-long plenum.

The plenum was fabricated from two copper blocks brazed together and then bored to accommodate a 5-inch-inside-diameter, 0.258-inch-thick copper pipe and four inlet ports having an inside diameter of 2.67 inches and a wall thickness of 0.165 inch. A 1/2-inch-wide annulus was provided in order to supply cooling water to the inlet ports and the inner wall. The upstream end of the plenum was capped with a 1/4-inch plate containing a support for a quartz window located 2 inches from

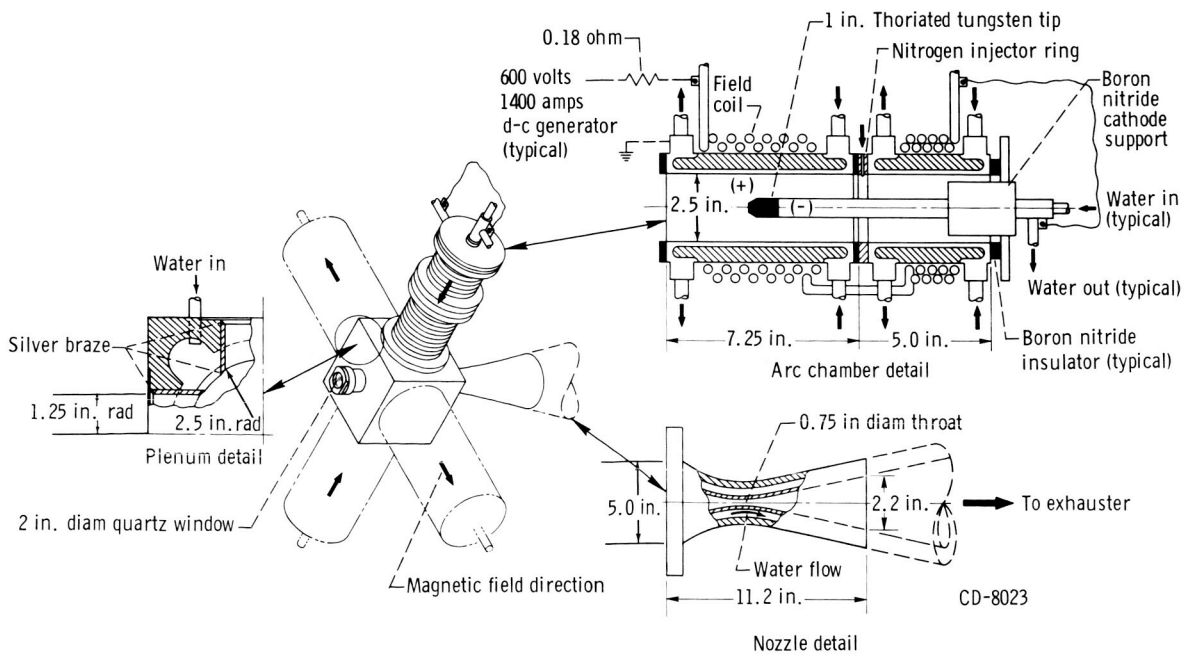


Figure 2. - Multiple-chamber arc heater configuration.

the inner wall. The quartz window support and upstream plate were cooled with a continuous winding of 1/4-inch copper tubing. The entire assembly was furnace brazed with a silver-copper compound that melts at 1435° F.

The electrodes consisted of a $2\frac{1}{2}$ -inch-inside-diameter, 7-inch-long water-cooled copper anode and a 1-inch-diameter, 2-percent-thoriated copper cathode with a tungsten tip. The magnetic field coil around the anode and cathode support chamber was made of 3/8-inch-diameter polyethylene-coated copper tubing and was connected electrically in series with the cathode. The direction of the induced magnetic field was reversed in adjacent heaters in order to avoid field cancellation (see fig. 2).

A conical nozzle, with a 3/4-inch diameter throat, a 15° divergence, and an 8.6 area ratio A/A^* was attached to the downstream end of the plenum. Eight splines along the length of the nozzle provided support for the inner wall as well as uniform spacing between the inner and outer walls. The inner wall was fabricated from beryllium copper with a gas-side plating of chrome 0.0005 inch thick. The plating protected the nozzle surface against impact from metallic particles occasionally ejected from the tungsten cathodes.

After approximately 4 hours accumulated running time, the first indication of plenum structural failure appeared in the form of porous water leaks through the copper inlet ports. These minute leaks were temporarily corrected by peening; however, one of the porous regions eventually ruptured, as shown in figure 3. Only the inlet ports exhibited this tendency to become porous. No apparent damage was incurred in the regions of the 5-inch inner wall or the quartz window.

The inlet ports represented a critical heat-transfer region because of their close

proximity to the arc. It is believed that the porosity in the inlet ports of the plenum was the result of abrupt expansions and contractions which occurred during each run cycle. (Approximately 60 runs were completed prior to the failure.)



Figure 3. - Heater plenum illustrating fractured inlet tube.

MEASUREMENTS AND INSTRUMENTATION

The performance evaluation of the multiple-chamber arc heater was based upon the computation of gas

power by a simple calorimetric technique in which the losses to the coolant are subtracted from the sum of the electrical input power and the small initial power in the gas before heating. Except for measurement inaccuracies, the error introduced in computing the gas enthalpy by this method results from radiation losses through the nozzle throat which were small at the pressure and energy levels investigated.

The following basic measurements were used to determine the multiple-chamber arc heater performance:

- (1) Arc voltage and current for each heater
- (2) Total nitrogen flow rate
- (3) Plenum pressure
- (4) Arc heater and nozzle cooling water flow rates and temperature rises

Other measurements, such as the total current and generator voltage, when used in conjunction with the value of the ballast resistance, provided an indirect means of checking the electrical characteristics of the arc. The plenum cooling-water flow rate and temperature difference were also measured in a few tests in order to separate the plenum loss from that of the electrodes.

Electrical Measurements

Voltmeters accurate to within 1 percent of full scale (750 volts) were used for direct reading of the arc voltages or the generator voltages alternately as selected by switching. Individual arc heater currents, as well as the total of the arc currents, were measured by means of calibrated shunts and read directly on ammeters accurate to within 1 percent of full scale (1500 amps). In addition to the direct readings, all arc voltages and all individual and total arc currents were recorded on a multichannel oscillograph. In studies of the electrical transients of the arc, the current was monitored on an oscilloscope.

Water and Nitrogen Flow Rates

Cooling water at a flow rate of about 300 gallons per minute at 250 pounds per square inch gage was supplied to the four arc chambers and the plenum. Of this total, approximately 40 percent was directed through the plenum and the remainder was divided among the four arc chambers. A nozzle coolant flow rate of 250 gallons per minute at 400 pounds per square inch gage provided throat coolant velocities of 140 feet per second.

Arc chamber and nozzle water flow rates were measured with calibrated orifice plates. A commercial differential-pressure sensor converted the orifice pressure drop into a flow-rate signal directly readable in units of gallons per minute. Plenum flow

rates were measured with a turbine-type flow transducer and counter.

The total gas flow rate to the four arc heaters was measured with a subsonic orifice plate providing differential pressures of 0 to 5 pounds per square inch for a constant upstream pressure of 500 pounds per square inch gage. The orifice pressures were converted to electrical signals and recorded on the oscillograph. Equal division of flow among the four arc heaters was achieved by matching the upstream pressures of critical-flow gas-injection rings.

Pressure

Pressure taps, which were located at the upstream end of each arc heater, were joined to a common manifold. The manifold pressure, representing an average arc chamber pressure, was measured with a 0- to 50-pound-per-square-inch differential transducer vented to the atmosphere. An oscillograph provided continuous recording of the chamber pressure. In cold flow tests, subatmospheric pressures were read on a 0- to 32-pound-per-square-inch absolute precision pressure gage. Exhaust pressures ranging from 0.1 to 2.0 torr were measured with a McLeod gage and dibutyl phthalate manometers incorporating a vacuum reference.

Temperatures

The temperature rise of the coolant for the arc heater (four arc chambers plus the plenum) ranged from 6° to 18° F, whereas that of the nozzle coolant ranged from 0.5° to 3° F. The relatively low magnitude of these temperature differences required an extremely accurate means of measurement. A precision self-balancing potentiometer and temperature convertor sensed the output of iron-constantan thermocouples and was used in conjunction with a system of thermopiles to monitor the water temperature rise for the various components. The iron-constantan thermocouples also provided an absolute measure of the reservoir water temperature, which increased by as much as 60° F in the course of an 8-minute test. The reservoir water temperature was used to correct the sensitivity factor for the thermopiles. In copper-constantan thermopiles of the type described in reference 7, the sensitivity factor changed by 0.016 millivolt per $^{\circ}$ F over the 60° F temperature range, which represents a 7-percent increase in output signal. A second type of thermopile, incorporating unshielded Chromel-constantan thermocouples produced a 6-percent increase in output signal over the same temperature range. Both types of thermopiles worked satisfactorily, having response times of about 1 second. Thermopile output signals were recorded on an oscillograph.

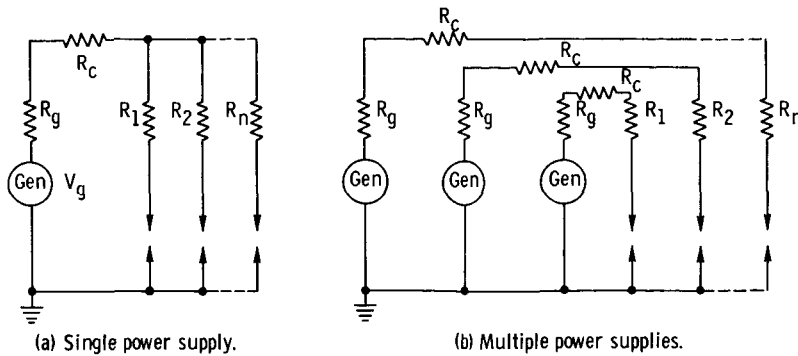


Figure 4. - Electric circuit connections.

PERFORMANCE

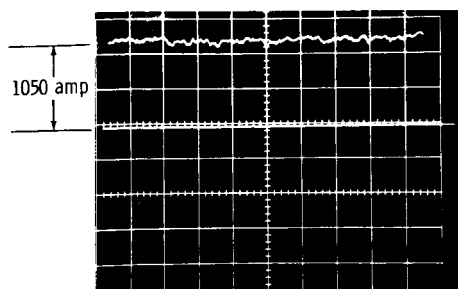
Electrical Stability Criterion

In a direct-current arc exhibiting a negative voltage-current characteristic, a stable discharge exists at the intersection of the generator load line and the arc discharge characteristic if the slope of the generator load line has a greater negative value than that of the discharge characteristic (ref. 8). This intersection becomes a stable operating point because deviations in the neighborhood of this point along the arc characteristic line create a difference between the applied voltage and the sum of the resistance drop and the arc voltage which will tend to return the current to the point of intersection. Oscillations about this stable point are normal, but it is desirable to minimize the amplitude of these fluctuations to lessen the possibility of arc blowout or burnout. In a system of multiple-arc discharges, each arc characteristic must satisfy the slope criterion. The direct-current power supplies had a flat voltage characteristic; therefore it was necessary to incorporate a ballast resistor in series with each arc to obtain a stable arc operating point. The arc current was controlled by adjusting the generator terminal voltage.

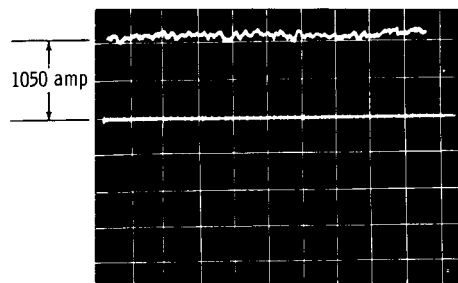
Parallel Circuits for Multiple-Heater Systems

Figure 4 illustrates two types of electric circuit connections that were examined in order to compare the differences in the electrical interactions of the discharges. These simplified circuits can be analyzed if circuit inductance and capacitance are ignored.

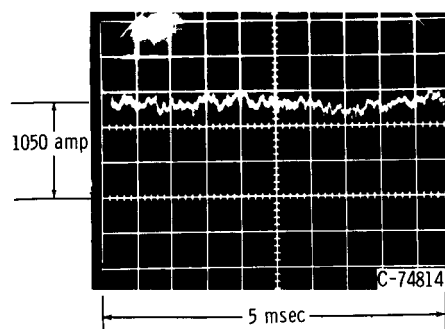
A single power supply (fig. 4(a)) is desirable from the standpoint of power supply and control simplicity; however, electrical coupling of the individual arc heaters takes place through the resistances R_g and R_c , which are common to all arcs. This cou-



(a) Field coil in series with arc. Generator voltage, 530 volts; arc voltage, 229 volts; ballast resistance, 0.2870 ohm.



(b) Field coil in series with arc. Generator voltage, 305 volts; arc voltage, 231 volts; ballast resistance, 0.0705 ohm.



(c) Field separately excited (reduction in series inductance). Generator voltage, 345 volts; arc voltage, 232 volts; ballast resistance, 0.1075 ohm.

Figure 5. - Oscilloscope traces showing arc current transients for different values of ballast resistance and series inductance.

pling causes fluctuations in any one arc heater to affect all the others.

With multiple power supplies (fig. 4(b)) no circuit resistances are common to the individual arc heaters, except the very low resistance ground return, and thus negligible coupling of the individual fluctuations occur. Experiments in which two arc heaters were connected to a single 500-volt, 6000-ampere, direct-current generator with $R_c = 0.08$ ohm and $R_1 = R_2 = 0.15$ ohm revealed the higher amplitude associated with this type of system than with separately connected discharges. These fluctuations, combined with the fluctuations in generator terminal voltage, confirmed the desirability of using independent power supplies.

Advantages of Inductive Reactance

The discharge fluctuations for each arc are influenced predominantly by the inductive reactance in the system rather than the resistance provided that sufficient resistance is available to meet the basic stability criterion mentioned previously. Operation at low values of ballast resistance is desirable from the standpoint of improving system efficiency, which can be defined as V_a/V_g . A system efficiency increase of 32 percent was achieved by reducing the ballast resistance from 0.2870 to 0.0705 ohm. Oscilloscope traces taken with these resistances are shown in figure 5(a) and (b). No change in fluctuation amplitude is evident.

In addition, several tests were made with the field coil surrounding the anode removed from the arc discharge circuit and separately excited with 1050 amperes from a welding generator. The resulting oscilloscope trace (fig. 5(c)) shows that the amplitude of the arc current oscillations increased when arc discharge circuit inductance was reduced in this manner.

As a result of these tests, each arc-heater field coil was connected in series with the arc. This series coupling, in addition to providing inductance, tends to protect the anode against burnout because the magnetic field is always present during arc operation.

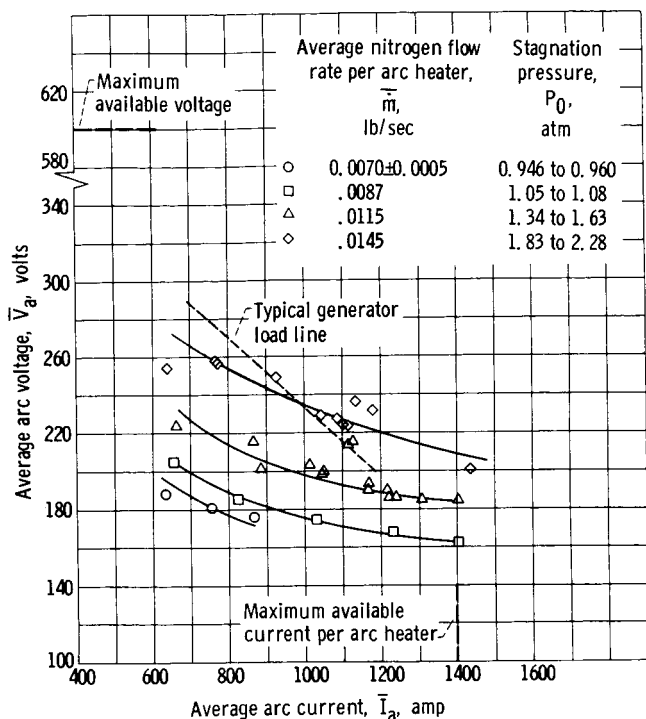


Figure 6. - Voltage characteristics of each arc heater in multiple-chamber configuration as function of flow rate. Ballast resistance, 0.18 ohm.

Since the available voltage exceeded the arc voltage, the amount of ballast resistance was based on a compromise between system efficiency and current control sensitivity. An experimentally derived resistance of 0.18 ohm provided the desired flexibility of operation with reasonable ballast power losses. At 1000 amperes, the ballast resistor power dissipation ranged from 43 to 50 percent of the total power depending upon the nitrogen flow rate.

Voltage Characteristics

The arithmetic average voltage-current characteristics of the four arcs in the heater are presented in figure 6, with the nitrogen flow rate as the param-

eter. The maximum difference in current among the four arcs was generally less than 50 amperes. The gas power, as well as the arc power, is continually changing with arc current; therefore, at constant flow rate, the stagnation pressure must also change (approximately as the square root of gas power). The stagnation pressures in figure 6 correspond to a total flow rate of four times the parametric values indicated. Since voltage-current characteristics depend strongly on arc heater configuration, caution should be observed in generalizing these data. The apparent scatter in the data results primarily from the inability to control the nitrogen flow rate precisely rather than from any measurement errors.

Upper and lower limits of arc voltage have not been established. The highest arc voltage occurred at the highest mass flow rate shown (0.0145 lb/sec per heater). Extended periods of operation at these conditions caused severe erosion of the insulating rings located between the anode and the plenum. Consequently, higher mass flows and higher voltages could not be run without danger of system failure.

A typical generator load line for a ballast resistance of 0.18 ohm and a generator terminal voltage of 415 volts is shown in figure 6. The lower limit of arc current depends upon the slope of the load line, which is dictated by the amount of ballast resistance. The minimum current required for maintenance of a stable discharge can be determined by establishing a parallel load line tangent to the arc characteristic. This

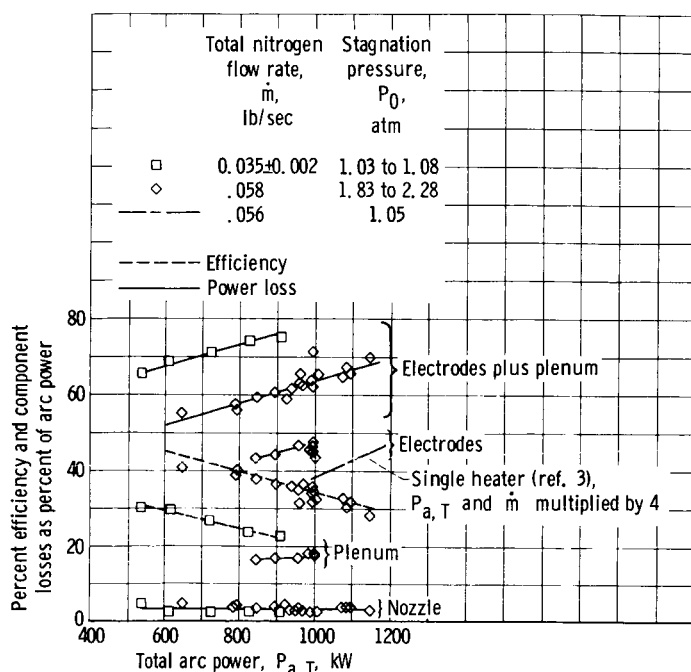


Figure 7. - Component losses and efficiency for multiple-chamber arc heater.

point occurs at approximately 600 amperes for a ballast resistance of 0.18 ohm. Although lower currents could be obtained by increasing the ballast resistance, operation in this regime was of little interest in the present study because of the low gas power and low system efficiency.

Energy Losses

Component fractional power losses and efficiencies are shown in figure 7 for an intermediate and a high total flow rate, 0.035 and 0.058 pound per second, respectively. The efficiency in figure 7 is based on the

losses to the electrodes, plenum, and nozzle and does not include power supply and ballast resistor losses. Also, the electrode losses of a single-arc chamber (ref. 3) are compared to those of the arc chambers in the multiple-heater system operating in a similar environment. In order to make a comparison in one figure between single- and multiple-chamber arc performance, the single-heater power and flow-rate data from reference 3 were multiplied by a factor of 4. If the stagnation pressure and flow rate were identical for the two cases, the curves representing the fractional power losses would be expected to coincide; however, the 0.75-inch-diameter throat of the multiple-chamber arc heater produced pressures slightly higher than those reported in reference 3 for a single heater operating with a 0.50-inch-diameter throat (nominal stagnation pressures of 2.0 and 1.0 atm, respectively). The slightly higher electrode power losses for the multiple system are attributed primarily to the higher stagnation pressure since the enthalpy levels were nearly equal for the two cases.

The plenum power losses are influenced by several factors, including anode geometry (ref. 9), degree of equilibrium, and the dynamics associated with gas interactions in the case of a multiple-arc system. Consequently, the determination of heat-transfer coefficients is a complex problem that does not easily yield to analysis. Measurements can be made of heat transfer from the plenum, however, and heat-transfer coefficients can be calculated from these measurements. In this study, plenum losses accounted for about 18 percent of the arc power at the high flow condition, 0.058 pound per second. At a power level of 1 megawatt, the average plenum heat-transfer rate was 178 Btu per

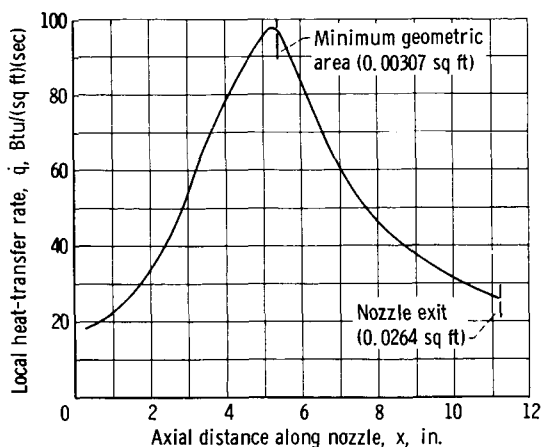


Figure 8. - Calculated nozzle heating rates. Stagnation enthalpy, 5500 Btu per pound; stagnation pressure, 2.0 atmospheres.

square foot per second.

Approximately 3 percent of the total input power was lost to the nozzle coolant. Measured nozzle heat loads ranged from 16 to 35 kilowatts over power levels of 530 to 1150 kilowatts. The error in these measurements could, however, be very large because the large quantity of cooling water produced a temperature rise of less than 1° F. Therefore, it was desirable to check the magnitude of the measured heat load by calculating the loss based on mean operating conditions of 5500 Btu per pound at 2.0 atmospheres. Calculations were based on the equation for forced

convection in laminar pipe flow (ref. 10)

$$\overline{Nu}_d = 3.65 + \frac{0.0668(d/x)Re_dPr}{1 + 0.04[(d/x)Re_dPr]^{0.667}}$$

In reference 11, this equation provided a good correlation between measured and theoretical heat loads on nozzles operating in similar environments. The low nozzle-throat Reynolds number (18 000) corresponding to the mean operating conditions tends to justify the use of laminar flow theory. The resulting heat-transfer profile is shown in figure 8. The maximum local heat-transfer rate, occurring slightly upstream of the minimum area, was approximately 100 Btu per square foot per second. The total heat loss was obtained by integrating the profile of local heat-transfer rates according to the following equation:

$$Q = \pi \int_0^L (\dot{q}/A)(d)dx$$

The total nozzle heat transfer, obtained by mechanical integration of the profile, was 18 kilowatts for the assumed stagnation conditions. This value, which is in reasonable agreement with the measurements, to some extent verifies the low magnitude of the nozzle heat loss (15.9 to 34.5 kW) at the conditions investigated.

The efficiency of the multiple-chamber arc heater shown in figure 7, ranged from 30 to 45 percent, the highest efficiency occurring at the lowest arc power and the highest flow rate.

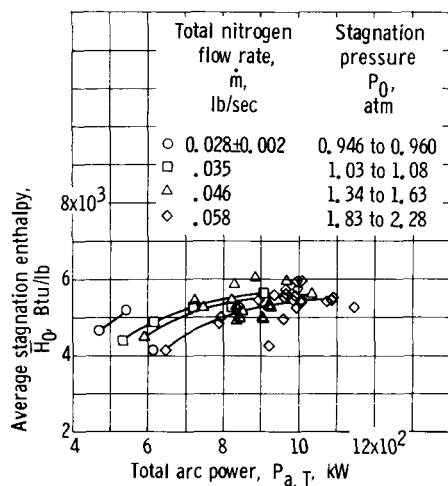


Figure 9. - Variation of stagnation enthalpy with arc power and flow rate. Single heater at reduced power. (Data from ref. 3.)

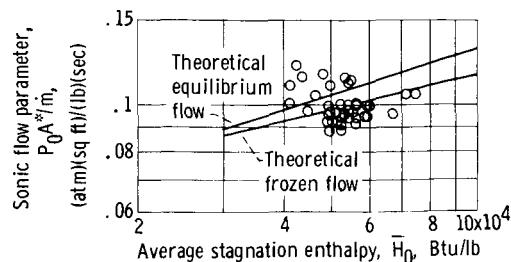


Figure 10. - Comparison of experimental and theoretical stagnation enthalpy using sonic-flow method of correlation.

Average Stagnation Enthalpy

The average stagnation enthalpy was determined from an energy balance of the heater-nozzle system according to the following equation:

$$\bar{H}_0 = H_i + \frac{P_{a,T} - (Q_E + Q_P + Q_N)}{\dot{K}m}$$

The stagnation enthalpy is plotted as a function of arc power and flow rate in figure 9. The stagnation enthalpy at constant flow rate increases with increasing arc power; however, the scatter in the experimental data makes the fairing of the curves difficult. Generally, the stagnation enthalpy was between 4000 and 6000 Btu per pound at stagnation pressures of 2.0 to 1.5 atmospheres, respectively.

The enthalpy levels obtained with the multiple-chamber arc heater were approximately the same as those reported in reference 3 for a single magnetically spun arc. The enthalpies are about the same for the two cases since the plenum fractional loss for the single heater was nearly the same as that of the multiple-heater system.

An attempt was made to correlate measured values of stagnation enthalpy by means of the sonic flow method (ref. 12), in which the flow is assumed to be one-dimensional, steady, homogeneous, isentropic, and in thermal equilibrium. For these assumptions, the sonic flow parameter $P_0 A^* / \dot{m}$ is approximately a logarithmically linear function of stagnation enthalpy at constant pressure. Theoretical values of $P_0 A^* / \dot{m}$ were computed from the nitrogen Mollier diagram of reference 13 and are shown in figure 10 for a stagnation pressure of 2.0 atmospheres. The theoretical frozen and equilibrium lines were used to bracket the flow parameter and thus serve as a guide to the accuracy of

measured values of stagnation enthalpy. These lines represent the upper and lower bounds of the flow parameter, and all measured values should lie within these limits if the initial assumptions of the analysis are not violated. As noted in figure 10, the majority of data fall outside the theoretical limits indicating the probability of departures from the ideal model and/or measurement errors. A discussion of some effects resulting from these departures is presented in references 12 and 14; however, measurements in this investigation were insufficient to determine the predominant reason for such behavior. Application of the pressure-rise technique of reference 12 for determining the stagnation enthalpy resulted in large discrepancies in experimental and theoretical values, which were attributed to differences in the flow discharge coefficient for cold and hot sonic flow. Cold-flow discharge coefficients as low as 0.6 were measured at the high flow rate, 0.058 pound per second, which indicated the presence of vortices in the plenum. Although measurements were inadequate to assess the values of hot discharge coefficients, it is expected, on the basis of references 14 and 15, that these values exceeded 0.9.

CONCLUSIONS

A multiple-chamber arc heater comprised of four direct-current arc heaters was tested over a range of power levels and nitrogen flow rates in order to ascertain the desirability of utilizing this type of configuration for powering hypersonic arc tunnels. Tests of the arc heater were concluded because a plenum failure occurred after an accumulated running time of 4 hours. Sufficient information was obtained, however, to reach the following conclusions:

1. The multiple-chamber arc heater provided a steady flow for running times up to 8 minutes at nominal stagnation conditions of 5500 Btu per pound and 2.0 atmospheres with a 3/4-inch-diameter nozzle throat.
2. Clustering of arc heaters provides a means of increasing gas power in direct proportion to the number of heaters if plenum losses are not included. The gas power could be predicted from single-heater data at simulated multiple-heater operating conditions if plenum losses could be estimated.
3. In a multiple-chamber configuration, the electrical fluctuations of the arcs are influenced by the type of power supply coupling. A separate power supply for each arc heater minimizes the system fluctuations. Individual arc fluctuations can be decreased by means of a series inductance; therefore, in the case of a magnetically spun arc it is desirable to maintain the field coil in series with the arc.
4. The enthalpy levels obtained with the four-chamber arc heater were approximately the same as those obtained with a single-arc heater of the same type operating

with a plenum at a slightly lower pressure level. The plenum fractional losses for the four-chamber arc heater were also about the same as that of the single chamber.

5. Since multiple-chamber arc heater systems are physically very complex, the minimum possible number of heaters should be used to attain a required power level. Chamber configurations other than the magnetically spun arc may be superior for use in a clustered system because of a higher gas power per arc.

Lewis Research Center,
National Aeronautics and Space Administration,
Cleveland, Ohio, April 12, 1965.

REFERENCES

1. Stine, Howard A. ; and Watson, Velvin R. : The Theoretical Enthalpy Distribution of Air in Steady Flow Along the Axis of a Direct-Current Electric Arc. NASA TN D-1331, 1962.
2. Shepard, Charles E. ; Watson, Velvin R. ; and Stine, Howard A. : Evaluation of a Constricted-Arc Supersonic Jet. NASA TN D-2066, 1964.
3. Boldman, Donald R. ; Shepard, Charles E. ; and Fakan, John C. : Electrode Configurations for a Wind-Tunnel Heater Incorporating the Magnetically Spun Electric Arc. NASA TN D-1222, 1962.
4. Rose, P. H. ; Powers, W. E. ; and Hritzay, D. : The Large High Pressure Arc Plasma Generator: A Facility for Simulating Missile and Satellite Re-Entry. Res. Rept. No. 56, Avco Corp., June 1959.
5. Bond, C. E. ; Cordero, J. ; Curtiss, H. A. ; and Henshall, B. D. : The Development of a Ten-Megawatt Multi-Arc and Its Operational Use in Hypersonic Re-Entry Vehicle Studies. Tech. Memo. No. RAD-TM-62-5, Avco Corp., Feb. 22, 1962.
6. Sheldon, John A. ; and Hunczak, Henry R. : An Analytical and Experimental Evaluation of a Two-Stage Annular Air Ejector for High-Energy Wind Tunnels. NASA TN D-1215, 1962.
7. Wald, David: Measuring Temperature in Strong Fields. Instr. and Control Systems, vol. 36, no. 5, May 1963, pp. 100-101.
8. Cobine, J. D. : Gaseous Conductors. Dover Pub., Inc., 1941.
9. Carden, William H. : Some Aspects of Energy Transfer in Electrode and Settling Sections of an Arc-Heated Wind Tunnel. AEDC-TDR-63-72, Aro, Inc., Apr. 1963.

10. Eckert, E. R. G. : Heat and Mass Transfer. Second Ed., McGraw-Hill Book Co., Inc., 1959.
11. Boatright, William B.; Stewart, Roger B.; and Grimaud, John E. : Description and Preliminary Calibration Tests of a Small Arc-Heated Hypersonic Wind Tunnel. NASA TN D-1377, 1962.
12. Winovich, Warren: On the Equilibrium Sonic-Flow Method for Evaluating Electric-Arc Air-Heater Performance. NASA TN D-2132, 1964.
13. Humphrey, R. L.; Little, W. J.; and Seeley, L. A. : Mollier Diagrams for Nitrogen. AEDC-TN-60-83, Arnold Eng. Dev. Center, May 1960.
14. Stewart, Roger B. : A Calorimeter Study of a Magnetically Stabilized Arc-Heater. AIAA J., vol. 2, no. 2, Feb. 1964, pp. 384-386.
15. Tempelmeyer, K. E.; and Rittenhouse, L. E. : Vortex Flow in Arc Heaters. AIAA J., vol. 2, no. 4, Apr. 1964, pp. 766-767.